Cellular Physiology and Biochemistry

Cell Physiol Biochem 2019;53:606-622
DOI: 10.33594/000000160
Published online: 25 September 2019
Accepted: 19 September 2019

Anne Dierks[a] Almke Bader[a] Tina Lehrich[a] Anaclet Ngezahayo[a,b]

[a]Department of Cell Physiology and Biophysics, Institute of Cell Biology and Biophysics, Leibniz University Hannover, Hannover, Germany, [b]Center for Systems Neuroscience (ZNS), University of Veterinary Medicine Hannover Foundation, Hannover, Germany

Connexin hemichannels • Adenosine receptors • Airway epithelium • Metabolite uptake • Calu-3 cells

Background/Aims: Adenosine release and connexin (Cx) hemichannel activity are enhanced in the respiratory epithelium during pathophysiological events such as inflammation. We analysed the interplay between Cx channels and adenosine signalling in human respiratory airway epithelium using the Calu-3 cell line as a model. ***Methods:*** The Cx hemichannel activity in Calu-3 cells was evaluated by dye uptake assays. The expressed Cx isoforms and adenosine receptor subtypes were identified by PCR and western blot analysis. Pharmacological and molecular biological experiments were performed to analyse the involvement of the different adenosine receptor subtypes, the induced signalling pathways and the contribution of specific Cx isoforms to the hemichannel activity. ***Results:*** The adenosine receptor agonist 5'-N-ethylcarboxamidoadenosine (NECA) increased the dye uptake rate in Calu-3 cells. The pannexon and Cx hemichannel inhibitor carbenoxolone (CBX) did not supress the dye uptake at pannexin-specific concentrations (100 µM). High CBX concentrations or the inhibitor La^{3+}, both effective on Cx hemichannels, were needed to inhibit the dye uptake. The NECA-related increase of dye uptake depended on enhanced cAMP synthesis and subsequent activation of the protein kinase A (PKA) as shown by quantification of cAMP levels and pharmacological inhibition of the adenylyl cyclase and the PKA. Further pharmacological inhibition as well as knockdown experiments with specific siRNA showed that the A_{2B} adenosine receptor was the subtype mainly responsible for the increased dye uptake. The NECA-related increase of the dye uptake rate correlated with a decrease of Cx43 mRNA and an increase of Cx26 mRNA content in the cells as well as Cx26 protein synthesis and was inhibited by Cx26 knockdown using Cx26 siRNA. Of note, a siRNA-induced knockdown of Cx43 increased the content of Cx26 mRNA

Anaclet Ngezahayo

Department of Cell Physiology and Biophysics, Institute of Cell Biology and Biophysics, Leibniz University Hannover, Herrenhäuser Straße 2, Hannover, 30419 (Germany)
Tel. +49 511 762 4568, Fax +49 511 762 2606, E-Mail ngezahayo@cell.uni-hannover.de

and correspondingly the dye uptake rate. ***Conclusion:*** The Calu-3 cell model shows that stimulation of the A_{2B} adenosine receptor subtype activates synthesis of cAMP. cAMP activates PKA and induces thereby an increase in Cx26 and a decrease in Cx43 mRNA levels. As a result, the synthesis of Cx26 is reinforced, leading to an enhanced Cx hemichannel activity. The report identifies a mechanism that integrates adenosine release and Cx hemichannel activity and shows how adenosine signalling and Cx channels may act together to promote persistent inflammation, which is observed in several chronic diseases of the respiratory airway.

Connexins (Cx) are membrane proteins that form gap junction channels and Cx hemichannels in the membrane of cells [1, 2]. They are the protein product of a gene family composed of 21 members in humans [2, 3]. As membrane proteins Cxs are synthesized and inserted into the membrane in the rough endoplasmic reticulum (ER). Along the trafficking pathway through the ER and Golgi apparatus, Cxs oligomerize to hexamers called connexons. These are transported to the plasma membrane where they form Cx hemichannels. Under normal conditions, the open probability of Cx hemichannels is very low due to the relatively high external Ca^{2+} concentration [4, 5]. Cx hemichannels of adjacent cells might dock to each other by interactions of specific motifs of their extracellular loops [6, 7] and form gap junction channels. Gap junction channels allow the intercellular exchange of ions and metabolites such as glucose and second messengers, e. g. cyclic nucleotides and IP_3 as well as oligonucleotides such as siRNAs or microRNAs. They thereby allow cells in tissues to form synchronized functional units as nicely illustrated in cardiac tissue [8]. When opened, Cx hemichannels are large enough to allow the exchange of metabolites with a size of 1-2 kDa between the external and the intracellular spaces. The Cx hemichannels might also participate in the release of mediators such as ATP, ADP or adenosine [9]. Before degradation or reuptake in the cells, the mediators can in a paracrine and autocrine manner bind to their receptors on cells in direct proximity of the site of release. The subsequently produced second messengers in the stimulated cells can then diffuse through gap junction channels, leading to a reaction in a large portion of the tissue. Thus, Cx channels as hemichannels and gap junction channels may participate in different signalling pathways such as adenosine signalling in tissues.

Adenosine is a metabolite ubiquitously present in tissue [10, 11]. As extracellular mediator, adenosine is either released or produced by rapid conversion of released ATP or ADP through a series of ectonucleotidases such as CD73 and CD39 [11, 12]. As in other tissue, the systemic basal adenosine concentration in respiratory tissue is in the range of 100 nM. However, local increases of external adenosine by transient adenosine and nucleotide release have been observed [13, 14]. The basal and transient adenosine level is part of the innate immune response and is involved in the general pulmonary physiology such as air surface liquid homeostasis [15–18]. Adenosine signalling is related to the adenosine receptor subtypes A_1, A_{2A}, A_{2B} and A_3 which are all linked to the adenylyl cyclase (AC) via G proteins [12]. While A_{2A} and A_{2B} adenosine receptors are linked to G_s proteins and activate cAMP synthesis, A_1 and A_3 adenosine receptors activate G_i proteins and inhibit cAMP synthesis [11, 12].

As locally released and produced mediator with a high degradation and reuptake rate, adenosine activates cells in close vicinity of its site of release. However, adenosine affects large tissue areas, suggesting a propagation of adenosine-dependent signalling through integrative mechanisms such as Cx channels [19]. Correspondingly, it was observed that pathological events, e. g. inflammatory reactions, the hallmark of various pathologies of the respiratory airway epithelium such as acute lung injury (ALI), chronic obstructive pulmonary disease (COPD), or asthma, correlated with an exacerbated adenosine release and changes in the activity of Cx channels in the whole organ [20–23]. The second messenger affected by adenosine signalling, cAMP, regulates various cellular processes by activating its targets,

the protein kinase A (PKA), the exchange protein directly activated by cAMP (Epac) [24] or cyclic nucleotide-gated (CNG) channels [25]. With respect to Cx channels, the cAMP/PKA cascade is a well-studied signalling pathway that predominantly increases the gap junction-dependent cell-to-cell communication [26, 27]. At molecular level, the cAMP/PKA cascade affects gap junction channels by phosphorylation of either Cxs [27, 28] or Cx-regulating proteins [29], leading to an increased insertion of connexons into the cell membrane, an elevated opening probability or an increased electrical conductance of single gap junction channels, as well as a reduced removal of gap junction channels from gap junction plaques. Additionally, activation of the cAMP/PKA cascade can upregulate Cx expression [29–32]. Finally, Bader et al. (2017) showed that in endothelial cells of the blood-brain barrier cAMP enhanced the gap junction coupling by activating a Ca^{2+} influx through CNG channels [25].

In order to analyse the interplay between adenosine signalling and Cx channels in epithelial cells of the respiratory airway system we used the Calu-3 cell line as model. These cells form a tight monolayer of polarized cells with a high transepithelial electrical resistance when cultured in transwell systems [33]. Calu-3 cells also express characteristic molecules of bronchial epithelial cells, such as cystic fibrosis transmembrane conductance regulator (CFTR), show a cAMP-dependent Cl^- secretion and are able to secrete pulmonary fluids with mucins and other immunologically active mediators [34, 35].

We found that the adenosine receptor agonist NECA reduced the mRNA level of Cx43 while increasing the mRNA amount of Cx26. The increased expression of Cx26 correlated with an enhanced Cx26 hemichannel activity. The effect of NECA was related to stimulation of the A_{2B} adenosine receptor subtype and depended on activation of a cAMP/PKA-dependent pathway.

Material

NECA and withaferin A were purchased from Biomol (Hamburg, Germany). MRS1754, SCH58261, BAY60-6583 and Lucifer Yellow (LY) were purchased from Sigma-Aldrich (Taufkirchen, Germany). CGS21680 was from Merck Millipore (Darmstadt, Germany). SQ22536 was from Enzo Life Sciences (Lörrach, Germany). Adenosine-3',5'-cyclic monophosphorothioate (Rp-cAMPS) was from Biolog Life Science Institute (Bremen, Germany). NECA, withaferin A, MRS1754, SCH58261, CGS21680, and BAY60-6583 were dissolved in DMSO while Rp-cAMPS and SQ22536 were dissolved in water. All inhibitors were preincubated for 30 min prior to addition of NECA. The vehicles DMSO or water were added to control cells in all experiments at maximal concentrations of 0.1% or 0.3%, respectively.

Cell Culture

The human lung adenocarcinoma epithelial Calu-3 cells (AddexBio, San Diego, CA, USA) were cultured in Dulbecco's MEM/Ham's F-12 medium (Biochrom, Berlin, Germany) supplemented with 10% foetal calf serum (Biochrom, Berlin, Germany), 1 mg/ml penicillin, and 0.1 mg/ml streptomycin (Biochrom, Berlin, Germany). The cells were maintained in a cell culture incubator in a humidified atmosphere with 5% CO_2 at 37°C. The cell culture medium was renewed every three days. Cells up to passage 35 were used for experiments.

Transepithelial electrical resistance (TEER) measurement

The TEER was monitored every 24 h by impedance spectroscopy using the cellZscope (nanoAnalytics, Muenster, Germany). For the measurements 10^5 Calu-3 cells/cm^2 were seeded in transwell inserts with a transparent PET membrane (pore size 0.4 µm, BD Falcon, Corning) and cultivated in cell culture medium for 3 days before being transferred into the cellZscope and placed in the cell culture incubator. TEER data were automatically recorded by the cellZscope software.

Western blot

Protein isolation was performed as described previously in Bader et al. (2017) [25]. For isolation of total proteins cells were grown in 60 mm diameter cell culture plates or 6 well plates. The cells were removed from the surface with a cell scraper, transferred in 1 ml PBS and centrifuged for 4 min at 900 × g at 4°C. The cell pellet was resuspended in 20 µl RIPA buffer (25 mM Tris HCl, pH 7.6, 150 mM NaCl, 1% nonidet P-40, 1% sodium desoxycholate, 0.1% SDS, freshly added 0.5% protease inhibitor cocktail (Roche, Waiblingen, Germany), 10 mM sodium fluoride, 1 mM sodium orthovanadate, 1.5 mM PMSF) and kept for 15 min on ice before centrifugation for 15 min at 14,000 × g at 4°C. Protein concentration was determined with a Bradford assay (Sigma-Aldrich) using bovine serum albumin (BSA) as standard. 20 µg total protein was mixed with 5 × Laemmli buffer (13 mM Tris HCl, 2% glycerol, 0.4% SDS, 0.002% bromophenol blue, 10 mM DTT, pH 6.8), heated at 70°C for 10 min and separated in 5% SDS-polyacrylamide stacking gels and 12% or 15% separation gels. Proteins were transferred onto a nitrocellulose membrane using a semi-dry blotting system (transfer buffer: 25 mM Tris HCl, pH 8.3, 192 mM glycine, 0.1% SDS, 20% methanol). The membranes were blocked in 5% non-fat dry milk powder in PBS containing 0.5% Tween 20 (PBS-T) for 2-3 h at room temperature. Anti-β-tubulin antibody as loading control (1:4,000, Sigma-Aldrich, T4026), anti-Cx26 antibody (0.5 µg/ml, Merck, MABT198), anti-Cx43 antibody (0.19 µg/ml, Sigma-Aldrich, C6219), anti-Cx45 antibody (1 µg/ml, Thermo Fisher Scientific, 41-5800), anti-claudin1 antibody (0.54 µg/ml, Thermo Fisher Scientific, 51-9,000), anti-claudin3 antibody (0.5 µg/ml, Thermo Fisher Scientific, 34-1700), anti-claudin4 antibody (1 µg/ml, Thermo Fisher Scientific, 32-9400), anti-claudin7 antibody (1.3 µg/ml, Sigma-Aldrich, SAB4500436), anti-A_{2A} adenosine receptor antibody (4 µg/ml, alomone labs, AAR-007), and anti-A_{2B} adenosine receptor antibody (3.75 µg/ml, alomone labs, AAR-003) were diluted in PBS-T and applied to the membranes at 4°C overnight. The secondary horseradish peroxidase-coupled anti-rabbit and anti-mouse antibodies (1:40,000 Sigma-Aldrich, A9169 and A9044) were each applied for 1 h at room temperature. The detection was carried out with a substrate containing coumaric and linoleic acid (100 mM Tris pH 8.5, 1.25 mM linoleic acid, 0.225 mM coumaric acid, freshly added 0.01% H_2O_2) and imaged with a CCD camera imaging system (Intas Science Imaging, Göttingen, Germany).

Immunofluorescence staining

For immunostaining 10×10^5 cells were seeded on collagen I-coated coverslips (diameter 5 mm) and grown for 48 h to a confluence of 70%. The cells were fixed with an acetone/methanol mix (1:1) for 5 min at -20°C and blocked with 1% BSA in PBS for 30 min at 37°C. The primary antibodies anti-Cx26 (2 µg/ml, Merck, MABT198), anti-Cx43 (0.75 µg/ml, Sigma-Aldrich, C6219), anti-Cx45 (10 µg/ml, Thermo Invitrogen, 41-5800), anti-claudin1 (5 µg/ml, Thermo Fisher Scientific, 51-9,000), and anti-claudin3 (60 µg/ml, Thermo Fisher Scientific, 34-1700) were diluted in PBS and added to the cells overnight at 4°C. The secondary iFluor488™-conjugated anti-rabbit and anti-mouse antibodies (AAT Bioquest, 16608, 16528) were diluted 1:1,000 in PBS with 2 µM DAPI (Sigma-Aldrich) for 1 h at 37°C. The cells were washed with PBS and stored at 4°C. Immunostaining was imaged with an Eclipse TE2000-E inverse confocal laser scanning microscope (Nikon GmbH) with a 60 x water immersion objective and the software EZ-C1 (Nikon GmbH).

Gold nanoparticle mediated laser perforation/dye transfer (GNOME-LP/DT)

GNOME-LP/DT experiments were performed as described previously in Begandt et al. (2015) [36]. The cells were seeded at a density of 1.5×10^5 cells/well in 96 multiwell plates and cultivated for 72 h until confluence. Gold nanoparticles (AuNPs, diameter 200 nm, 0.5 µg/cm^2) were added 3 h before an experiment started. Cells were washed with a bath solution containing 121 mM NaCl, 5.4 mM KCl, 6 mM $NaHCO_3$, 5.5 mM glucose, 0.8 mM $MgCl_2$, 1 mM EGTA, and 25 mM HEPES (pH 7.4, 295 mOsmol/l). The laser permeabilisation was performed in presence of 0.25% LY dissolved in bath solution. The laser system set-up and laser treatment parameters were according to Heinemann et al. (2013) [37]. The set-up included a 532 nm Nd:YAG microchip laser (Horus Laser, Limoges, France), enabling 850 ps laser pulses with a repetition rate of 20 kHz, a telescope for the adjustment of the laser diameter and a halfwave plate combined with a polarizing beam-splitter (Thorlabs, Newton, USA) for adjustment of the laser power. A motorised stage (Carl Zeiss, Jena, Germany) with controller unit (Prior Scientific, Cambridge, UK) and a scanner (Müller Elektronik, Spaichingen, Germany) enabled the positioning and scanning of the multiwell plates. The laser power and the scanning velocity as well as the selection of wells were controlled by a custom-made LabView-based software [37]. To perform GNOME LP/DT, in each well of a 96 multiwell plate, a line of cells

was optoperforated by a 20 mW laser beam with a diameter of 60 µm and a scanning velocity of 60 mm/s. After 10 min dye diffusion time, the cells were washed with Ca^{2+}-containing bath solution as previously described. The cells were fixed with 4% formaldehyde. In CBX experiments, 400 µM CBX was present during optoperforation and all washing steps. To automatically document the GNOME LP/DT experiments, images were obtained with an Orca Flash 4.0 camera (Hamamatsu Photonics, Herrsching am Ammersee, Germany) mounted onto an Eclipse Ti microscope (Nikon) with a 10 x objective using the NIS elements AR 4.21 software (Nikon). The tool Multipoint ND acquisition was used to generate three images with 2044 × 2048 pixels (1348.4 × 1351.04 µm) per well along the perforated fluorescent cell band plus one image aside for background subtraction. To analyse the diffusion distance in the fluorescence plot profiles, a Java-based ImageJ plugin was used which included a background subtraction. The results were passed to Octave 4.0-based software for calculation of the dye diffusion distances. The results are given as mean ± SEM from at least three biological replicates, the significance of the mean difference was evaluated by a student's *t* test.

Dye uptake assays

The activity of Cx hemichannels was analysed by measuring the ethidium bromide (Etd) uptake slightly modified from Schadzek et al. (2019) [38]. Calu-3 cells and HeLa cells were cultivated to 40% confluence on collagen I-coated coverslips. The cells were placed in a perfusion chamber with a chamber volume of approximately 400 µl and mounted on an Eclipse Ti microscope (Nikon). Regions of interest (ROIs) were selected in a transmission micrograph of the cells acquired with an Orca flash 4.0 CCD camera (Hamamatsu Photonics Germany). During the experiment, fluorescent images were taken every 15 s with an exposure time of 900 ms to assess fluorescence intensity changes within the ROIs using the NIS-Elements AR 4.4 software (Nikon GmbH). The ISMATEC REGIO ICC peristaltic pump (Cole-Parmer GmbH, Wertheim, Germany) controlled by the software ISMATEC® Pump Control (Cole-Parmer GmbH) was used to maintain a constant 1 ml/min medium flow rate. During the first 5 min of a 20 min long dye uptake experiment, the cells in the chamber were perfused with a prewarmed (37°C) bath solution containing 121 mM NaCl, 5.4 mM KCl, 6 mM $NaHCO_3$, 5.5 mM glucose, 0.8 mM $MgCl_2$, 1 mM EGTA, and 25 mM HEPES (pH 7.4, 295 mOsmol/l), and 5 µM ethidium bromide. For the next 10 min, the medium was changed to a Ca^{2+}/Mg^{2+}-free solution. In some experiments, cells were additionally perfused for 5 min with 100 µM, 400 µM CBX or 1 mM La^{3+} added to the Ca^{2+}-free solution. The dye uptake rate (Etd uptake in AU/min) was calculated from minute 1.5-2.5, 5.5-7.5, and 15.5-17.5. The significance of the differences of different perfusion solutions was evaluated by student's *t* test.

RT-PCR

For RT-PCR the PeqGOLD Total RNA kit (Peqlab, Erlangen, Germany) was used for total RNA isolation of cells grown on tissue culture plates according to the manufacturer's protocols. The RNA was eluted twice from the spin columns with 20 µl prewarmed (56°C) RNase-free water. The RNA concentration was measured with a Nanodrop2000c™ spectrophotometer (Peqlab). The Maxima First Strand cDNA synthesis kit for

List of all primer pairs used for PCR and quantitative real time PCR

RT-qPCR with dsDNase (Thermo Fisher Scientific) was used for cDNA synthesis. Up to 5 µg total RNA were incubated with 1 µl dsDNAse and 1 × dsDNAse buffer for 30 min at 37°C. 1 × reaction buffer and 2 µl enzyme mix were added in a final volume of 20 µl. The reaction was carried out for 10 min at 25°C, 30 min at 65°C and 5 min at 85°C. Complete removal of genomic DNA was confirmed before reverse transcription by PCR analysis. The primer pairs for gene expression analysis of Cx isoforms and adenosine receptor subtypes are given in Table 1. PCR analyses for qualitative gene expression assessment were performed with the OneTaq® Quick-load mastermix (New England Biolabs). Quantitative real time PCR was used to quantify gene expression changes after NECA treatment and to analyse RNA knockdown after siRNA transfection. The glyceraldehyde 3-phosphate dehydrogenase (gapdh) and β-actin (actB) genes were used as housekeeping genes for normalization. The ΔΔct method was used for quantification of the relative mRNA amounts. The real time PCR was performed with the KAPA SYBR™ FAST Universal mastermix (Kapa Biosystems) in the peqSTAR 96Q real time PCR cycler (Peqlab) and was carried out with an initial denaturation at 95°C for 3 min, 40 cycles of denaturation at 95°C for 15 s and annealing of primers and elongation at 60°C for 30 s, followed by melt curve generation.

Measurement of intracellular cAMP levels

For ELISA experiments 0.5 × 10^6 cells per well were seeded in a 24 multiwell plate and grown for 5 days until confluent. Cells were treated for 20 min with 10 µM NECA or vehicle control (0.1% DMSO). Measurements of cAMP levels were performed using the cAMP ELISA Kit (Cayman Chemical, 581001) according to the manufacturer's protocol. For cell lysis 100 µl of 0.1 M HCl were added per well for 20 min at room temperature before the lysate was centrifuged at 1,000 x g for 10 min. The supernatant was used as samples for the assay. The luminometric measurement was performed with a multiplate reader (Mithras, Berthold) with a measurement time of 1 s per well. Defined cAMP concentrations served as standard. Chemiluminescence values of treated cell samples were normalised to control cell samples. The results are given as mean ± SEM from at least two different cell passages. The significance of the difference was evaluated by student's *t* test.

Knock-down of connexin isoforms and the A_{2B} adenosine receptor subtype

For siRNA-mediated knockdown of Cx isoforms and the A_{2B} adenosine receptor subtype, 30 × 10^5 cells/cm^2 were seeded on collagen I-coated coverslips and grown for 24 h to a confluence of about 30%. Cell culture media was changed to Opti-MEM (Thermo Fisher Scientific). Cx26-siRNA (Qiagen, Hilden, Germany, SI03047856), Cx43-siRNA (SI02780491), A_{2B} adenosine receptor-siRNA (SI02662982), and Silencer Select Negative Control No. 2 siRNA (Thermo Fisher Scientific) were diluted in JetPrime dilution buffer (Polyplus transfection, Illkirch, France) to a final siRNA concentration of 9.6 nM per 48-well and 26.4 nM per 24-well. Per 48-well 1 µl, per 24-well 1.5 µl JetPrime transfection reagent (Polyplus transfection) were added. The transfection mix was incubated for 15 min at room temperature before addition to the cells. After 6 h the transfection medium was replaced by standard cell culture medium and cells were cultivated for 48 h before dye uptake experiments or quantification of mRNA amount was performed.

Cx channels in Calu-3 Cells

Calu-3 cells form a barrier characterised by a TEER of 500–2,000 Ω cm^2 [39] and are therefore considered as an adequate model for the respiratory epithelium. We used this cell model to analyse the interaction between Cx channels and adenosine signalling in the airway respiratory epithelium. Plated at a density of 10^5 cells/cm^2, Calu-3 cells formed a monolayer with a TEER of about 700 Ω cm^2 within about 11 days (Fig. 1A). This TEER value correlated with the expression of claudins, as shown by western blotting for Cld1, Cld3, Cld4 and Cld7 (Fig. 1B). Moreover, immunocytochemistry showed the presence of claudins distinctively located at cell-cell contact regions (Fig. 1C).

Concerning Cx channels, GNOME-LP/DT experiments showed that Calu-3 cells were coupled by gap junction channels. In Calu-3 cell monolayers, a LY-positive cell band (Fig. 2A) of about 170 µm (Fig. 2B) was found after GNOME-LP treatment. Applied in presence

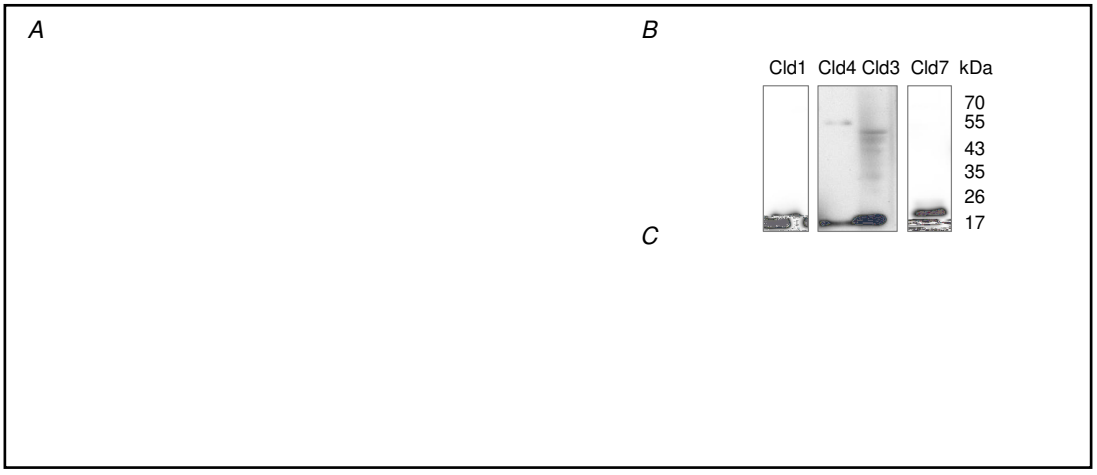

Calu-3 cells cultivated in transwell inserts formed a tight barrier. (A) Time course of TEER development recorded with the cellZscope for cells cultivated in transwell inserts. The data points represent the average ± SEM from three independent experiments. The red line represents a fitting of the data points to the Boltzmann equation. (B) Expression of the claudin (Cld) isoforms Cld1, Cld3, Cld4, and Cld7 in Calu-3 cells shown by western blotting. (C) Immunofluorescence staining shows intercellular membrane localisation of Cld1 and Cld3. The scale bar represents 20 µm.

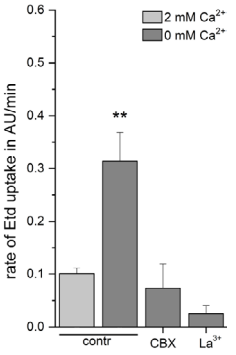

Gap junction coupling and Cx hemichannel activity in Calu-3 cells. (A) Representative micrographs of Calu-3 cells after GNOME-LP/DT experiments performed in absence or presence of the gap junction channel inhibitor carbenoxolone (CBX). The scale bar represents 200 µm. (B) The quantification of the experiments showed that CBX reduced the dye diffusion distance of LY from about 170 µm to about 110 µm. The results are shown as average ± SEM from twenty experiments with five cell culture passages. The data were statistically compared using student's t test (P<0.001 ***). (C) Time course of a dye uptake experiment showed that reduction of the external Ca^{2+} concentration accelerated the dye uptake as shown by the slope of the tangent to the dye uptake curve (red line). (D) Quantification of dye uptake experiments showing that various inhibitors of Cx hemichannels inhibited the dye uptake. The results are shown as average ± SEM of five experiments with three cell culture passages. The data were statistically compared using student's t test (P<0.01 **).

of the gap junction inhibitor CBX (Fig. 2A) GNOME-LP generated a LY-positive cell band of only 110 µm (Fig. 2B), indicating that the wider band of LY-positive cells observed in absence of CBX was due to lateral diffusion of LY through gap junction channels between the cells.

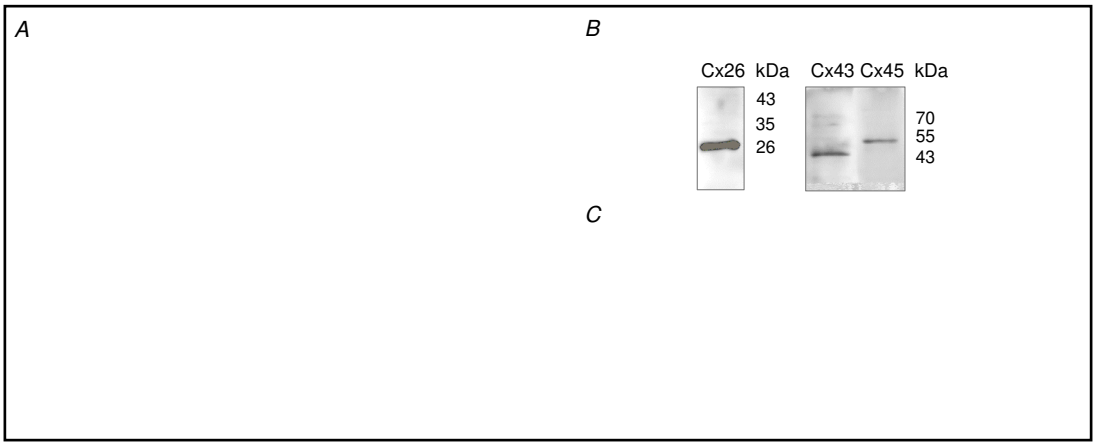

Expression of connexion isoforms in Calu-3 cells. (A) RT-qPCR experiments showed expression of different Cx isoforms. Cx43 and Cx45 were remarkably high expressed, followed by Cx26. The results represent the average ± SEM from three experiments with three cell culture passages. (B) Western blots confirmed protein synthesis of Cx26, Cx43 and Cx45. (C) In immunostainings Cx26, Cx43, and Cx45 were also found at cell-cell contact regions. The scale bar represents 20 µm.

In addition to gap junction channels, Cxs also form hemichannels that, when open, allow the exchange of metabolites between the intracellular and extracellular spaces [9]. The hemichannels can be analysed by following the uptake of membrane impermeable dyes such as ethidium bromide (Etd) [5, 38]. In comparison to HeLa cells which are almost Cx-free and thus did not show dye uptake (Fig. 2C), Calu-3 cells cultivated under control conditions were able to absorb Etd 3 times as effective when the Ca^{2+} concentration in the external solution was strongly reduced (Fig. 2C, D). The uptake of Etd was inhibited by gap junction inhibitors such as 400 µM CBX and 1 mM La^{3+} below the control level with an Etd uptake rate of 0.1 Au/min (Fig. 2C, D), but was not affected by low concentration (100 µM) of CBX (Supplementary Fig. S1 – for all supplementary material see www.cellphysiolbiochem.com). With respect to the expressed Cx isoforms, RT-qPCR revealed the expression of Cx26, Cx30, Cx32, Cx37 as well as Cx46 and, more pronounced, Cx43 and Cx45 (Fig. 3A). At protein level, western blot experiments confirmed protein expression of Cx26, Cx43 and Cx45 (Fig. 3B). Similarly, the presence of Cx26, Cx43 and Cx45 localised at cell borders between adjacent cells was observed in immunocytochemical experiments (Fig. 3C).

Interplay between adenosine receptors and Cx channels

To analyse whether adenosine signalling affected the Cx channels in Calu-3 cells, the cells were cultivated in presence of the adenosine receptor agonist NECA. The analysis of gap junction coupling and Cx hemichannels with GNOME-LP/DT and dye uptake experiments, respectively, showed that NECA affected both the cell-cell coupling through gap junction channels and the dye uptake through Cx hemichannels. While incubation of Calu-3 cells with 10 µM NECA for 24 h significantly reduced the gap junction-dependent dye transfer by half (Supplementary Fig. S2), the Cx hemichannel-dependent dye uptake rate was significantly enhanced by nearly 50% (Fig. 4A). The influence of adenosine signalling on gap junction channels will not be followed in detail in this study. The present report aims to analyse how stimulation of adenosine receptors might affect the activity of Cx hemichannels in respiratory epithelial cells. Therefore, we first analysed the expression of adenosine receptor subtypes. RT-PCR experiments showed the expression of the adenosine receptor subtypes A_{2A} and A_{2B} (Fig. 4B) while the subtypes A_1 and A_3 could not be detected. Western blot experiments confirmed the presence of A_{2A} and A_{2B} adenosine receptors on protein level (Fig. 4B). The qRT-PCR analysis revealed a more than 10-fold higher mRNA level of the A_{2B} adenosine receptor subtype in comparison to the A_{2A} adenosine receptor subtype (Fig. 4B). A_{2A} and A_{2B} adenosine receptors are both coupled to G_s proteins [12]. Accordingly, the Calu-3 cells responded to

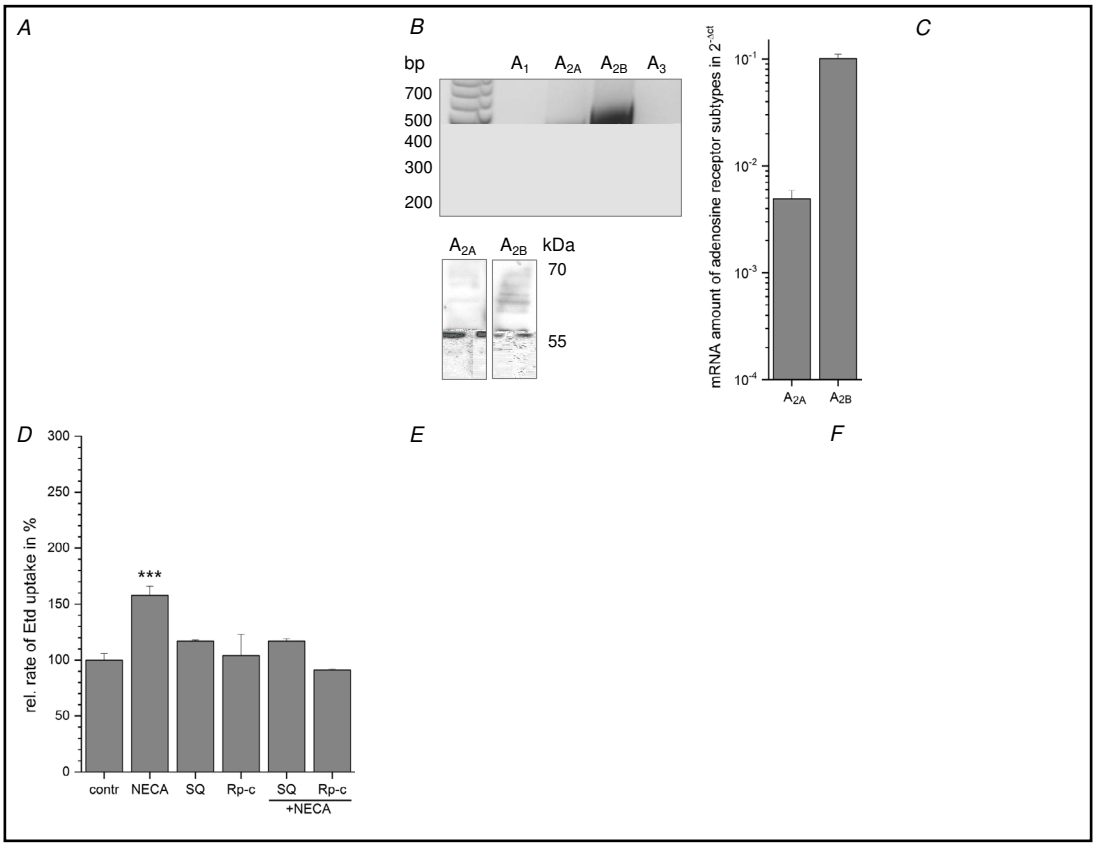

Expression of adenosine receptor subtypes in Calu-3 cells. (A) Increase in the dye uptake rate induced by NECA (10 µM, 24 h) as quantified from dye uptake experiments. (B) RT-PCR analysis and western blot experiments showed expression of the adenosine receptor subtypes A_{2A} and A_{2B}. qRT-PCR analysis showed a remarkably higher expression of the A_{2B} adenosine receptor subtype. The results are given as average ± SEM from three cell culture passages. (C) NECA increased the intracellular cAMP concentration. The results are given as average ± SEM from three cell culture passages. (D) The increase in the dye uptake rate was attenuated by the AC inhibitor SQ22536 (SQ, 400 µM) and the PKA inhibitor Rp-cAMPs (Rp-c, 200 µM). (E) The NECA-induced increased dye uptake rate was not significantly affected by the A_{2A} adenosine receptor antagonist SCH58261 (SCH, 0.5 µM). The A_{2B} adenosine receptor antagonist MRS1754 (MRS, 0.5 µM) blocked the NECA-induced increase in the dye uptake rate. The A_{2A} adenosine receptor-specific agonist CGS21680 (CGS, 50 nM) did not change the dye uptake rate, while the A_{2B} adenosine receptor-specific agonist BAY60-6583 (BAY, 100 nM) significantly increased the dye uptake rate. (F) siRNA-knockdown of the A_{2B} adenosine receptor subtype blocked the NECA-induced increase in the dye uptake rate. The dye uptake rates are given as average ± SEM from respectively six experiments with three cell culture passages. The data were statistically compared to the control using student's t test (P<0.05 *, P<0.01 **, P<0.001 ***).

NECA by increasing the intracellular cAMP concentration by about 50% compared to control conditions (Fig. 4C). This increase in cAMP was also responsible for the NECA-dependent enhanced dye uptake since application of SQ22536, a general inhibitor of AC, supressed the NECA-induced increase in dye uptake to an only 17% higher relative Etd uptake compared to the control (Fig. 4D). Further pharmacological inhibition of A_{2A} and A_{2B} adenosine receptors using SCH58261 (0.5 µM) and MRS1754 (0.5 µM), respectively, had different effects on the NECA-related enhancement of the dye uptake. While SCH58261 did not affect the NECA-induced enhancement of dye uptake with a 55% higher relative Etd uptake, MRS1754 as inhibitor of the A_{2B} adenosine receptor subtype antagonized the NECA-dependent increase in dye uptake to an with only 18% negligibly higher relative Etd uptake compared to control conditions (Fig. 4E). Inversely, CGS21680 (50 nM), a specific agonist of A_{2A} adenosine

receptors, was not able to significantly increase the dye uptake with a 23% higher relative Etd uptake, while BAY60-6583 (0.1 µM), a specific agonist of the A_{2B} adenosine receptor subtype, was similarly efficient in increasing the dye uptake rate as NECA with a 80% higher relative Etd uptake compared to the control (Fig. 4E) [40]. Additionally, the NECA-related increase in the dye uptake was suppressed by knockdown of the A_{2B} adenosine receptor subtype with specific siRNA with 90% relative Etd uptake compared to the control (neg siRNA) (Fig. 4F). Taken together, the results suggest that NECA increased the dye uptake in Calu-3 cells by activating the A_{2B} adenosine receptor subtype which subsequently activated cAMP synthesis (Fig. 4C). cAMP is a second messenger which mostly acts via activation of the PKA. We therefore analysed a possible involvement of the PKA. As shown in Fig. 4D the PKA inhibitor Rp-cAMPs (200 µM) antagonized the NECA-induced increase in dye uptake to control level (90% rel. Etd uptake compared to control conditions), suggesting a central role for the PKA in the regulation of Cx hemichannels.

Contribution of specific Cx isoforms to the hemichannel activity

At Cx level, qRT-PCR revealed that NECA increased the mRNA levels of Cx26 and Cx30 by about 50% and decreased the content of Cx43 mRNA (0.79 rel. mRNA amount compared to the control) but did not significantly affect the Cx45 mRNA level (1.20 rel. mRNA amount compared to the control) (Fig. 5A). Accordingly, Cx26 was increased at protein level by approximately 2.6-fold (Fig. 5B). Moreover, western blot experiments also showed that NECA decreased the expression of Cx43 at protein level to 62% of control levels (Fig. 5B). It can therefore be assumed that the NECA-related increase of the dye uptake rate was mostly related to an increase of the cellular Cx26 mRNA content and upregulation of protein synthesis of Cx26 (Fig. 6). This assumption agrees very well with the observation that the PKA inhibitor Rp-cAMPs, which was able to suppress the NECA-related enhancement of dye uptake, also suppressed the NECA-related upregulation of the Cx26 mRNA level to control level (0.94 rel. mRNA amount compared to the control) (Fig. 5A). Furthermore, inhibition of the specificity protein 1 (Sp1), a transcription factor for Cx26, with withaferin A concomitantly with the application of NECA completely suppressed an increase of Cx26 transcript levels (1.02 rel. mRNA amount compared to the control) (Fig. 5A). This suggests a prominent role of the Sp1 transcription factor in the NECA-induced cAMP/PKA cascade (Fig. 6).

The prominent role of Cx26 in dye uptake was further confirmed by knockdown of Cx26 using Cx26-siRNA (Fig. 5C, Supplementary Fig. S3). The specific siRNA decreased the dye uptake rate by about 55% (Fig. 5D). In comparison, a Cx43-siRNA did not reduce the dye uptake but rather showed a tendency to increase the dye uptake rate to 154% compared to the control siRNA (neg siRNA) (Fig. 5D). Moreover, in cells treated with Cx26-specific siRNA, NECA was not able to enhance the dye uptake rate anymore (40% rel. Etd uptake compared to the neg siRNA) (Fig. 5D). This effect was due to a specific targeting of Cx26 since a control siRNA not targeting Cxs (Fig. 5C) was not able to affect the NECA-related enhancement of dye uptake with an 80% higher relative Etd uptake compared to the control (neg siRNA) (Fig. 5D). When using the Cx43-siRNA, the Cx26 mRNA level was increased by 1.4-fold (Fig. 5C). The results suggest that NECA, by activating A_{2B} adenosine receptors, induced a cAMP/PKA cascade that upregulated the expression of the Cx26 isoform via the Sp1 transcription factor, which in turn upregulated the formation of Cx hemichannels responsible for the enhanced dye uptake rate in Calu-3 cells (Fig. 6).

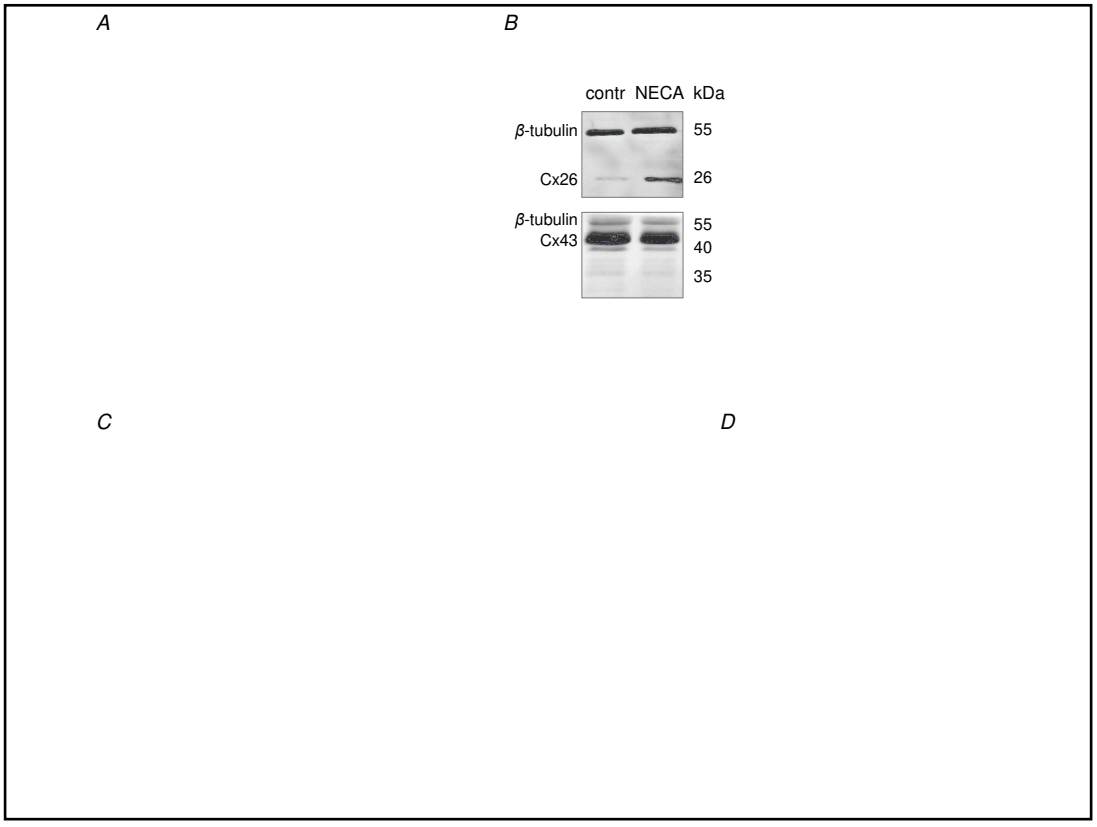

Activation of adenosine receptors regulates connexin expression in Calu-3 cells. (A) qRT-PCR analysis showed an increase in the mRNA level of Cx26, Cx30 and a decrease in the mRNA level of Cx43 induced by NECA (10 µM, 24 h). The PKA inhibitor Rp-cAMPs (Rp-c, 200 µM) as well as the Sp1 inhibitor withaferin A (witA, 1 µM) blocked the NECA-induced increase in Cx26 mRNA. (B) Western blot experiments showed an increase in Cx26 protein level and a decrease in Cx43 protein level induced by NECA. The results are given as average ± SEM from three cell culture passages. (C) The mRNA levels of Cx26 and Cx43 were significantly reduced after 48 h treatment with specific siRNAs. The Cx26 mRNA level was increased after Cx43-siRNA treatment, the Cx30 mRNA level was not significantly affected by both Cx26- and Cx43-siRNAs. The results are given as average ± SEM from at least three experiments. (D) The dye uptake rate of Calu-3 cells was significantly reduced after knockdown of Cx26 with specific siRNA, and NECA was not able to affect it. The results are given as average ± SEM from at least six experiments with three cell culture passages. The data were statistically compared to the control (contr, neg siRNA) using student's t test ($P<0.05$ *, $P<0.01$ **, $P<0.001$ ***).

Pulmonary epithelial cells maintain a barrier that separates the atmospheric space (luminal) from the body circulatory system (abluminal) [41]. The physiological function of this barrier is modulated by different mediators such as adenosine which is released by different cells in the tissue [22, 42]. The systemic concentration of adenosine is maintained at very low levels by mechanisms of cellular uptake and degradation [43]. However, transient and local adenosine increases can be observed in response to various stimuli within the tissue and it was observed that locally released adenosine can affect the function of a whole organ [14], suggesting an involvement of integrative systems such as Cx channels [19]. In the present report Calu-3 cells were used as model to analyse the interplay between adenosine signalling and Cx channels in human respiratory airway epithelial cells. As shown above, Calu-3 cells formed an excellent barrier characterized by a high TEER (Fig. 1A). This barrier,

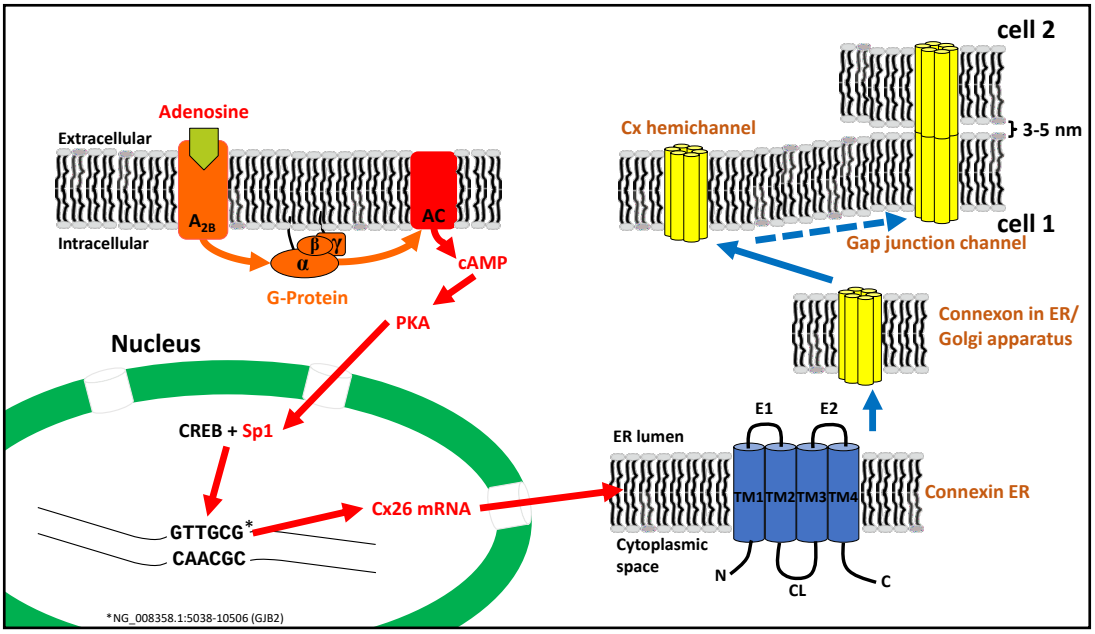

Proposed mechanism of interplay between adenosine signalling and Cx26 hemichannels. The stimulation of A_{2B} adenosine receptors induces the synthesis of cAMP which activates the protein kinase A (PKA). The PKA in turn phosphorylates CREB and/or the specificity protein 1 (Sp1) resulting in an upregulation of Cx26 expression and synthesis. A proposed enhanced insertion of Cx hemichannels into the membrane leads to an increase in Cx hemichannel activity. Red labels indicate experimental confirmations.

which is one of the convincing evidences that Calu-3 cells are a suitable model for epithelial cells of the respiratory airway [33], correlated with an expression of the claudins Cld1, Cld3, Cld4, and Cld7 (Fig. 1B). These were detected in western blot experiments (Fig. 1B) as well as in immunocytochemical experiments with a prominent localisation at cell-cell borders (Fig. 1C) where they probably participated in tight junction formation [44].

Adenosine receptors are part of the purinergic signalling system, which is linked to a regulation of diverse functions in the respiratory epithelium [9, 13–16]. In our experiments we found that a 24 h treatment of Calu-3 cells with NECA, an agonist that stimulates both A_{2A} and A_{2B} adenosine receptor subtypes [40], reduced the gap junction coupling-related dye transfer (Supplementary Fig. S2) but increased the dye uptake (Fig. 4A). In the following we concentrated on the dye uptake results. Dye uptake can be achieved by activation of various channels such as pannexons formed by pannexins, P2X7 channels or Cx hemichannels called connexons [45]. At pharmacological level, connexons and pannexons are inhibited by agents such as CBX or La^{3+}, but differ with respect to their sensitivity to these agents. Pannexons are already closed at low micromolar CBX concentrations while higher concentration of CBX or La^{3+} are needed for a proper inhibition of connexons [5, 46]. In our experiments we found that the dye uptake was only affected by 400 µM CBX and 1 mM La^{3+} (Fig. 2C, D and Fig. 4A). CBX concentrations of 100 µM did not affect the dye uptake rate (Supplementary Fig. S1). Taken together, these findings show that the dye uptake was related to Cx hemichannels.

NECA is an agonist of adenosine receptors that regulate cAMP synthesis by activation or inhibition of the AC. In our experiments, the NECA-related enhancement of dye uptake was accompanied by an increase of cAMP synthesis (Fig. 4C) and was suppressed by inhibition of the AC with SQ22536 (Fig. 4D), indicating that NECA affected the dye uptake by activating A_{2A} and A_{2B} adenosine receptors that stimulate the AC to synthesize cAMP. This is supported by the expression analysis that revealed that Calu-3 cells only expressed the A_{2A} and A_{2B} adenosine receptor subtypes (Fig. 4B). At mRNA level, adenosine receptor stimulation increased the cellular content of Cx26 and Cx30 mRNA (Fig. 5A) and we could also observe that Cx26 was upregulated at protein level as shown by western blotting

(Fig. 5B). Moreover, the dye uptake and its adenosine receptor-related enhancement were completely inhibited when Cx26 was knocked down using Cx26-specific siRNA (Fig. 5D). The data stress the prominent role of Cx26 in the formation of Cx hemichannels and in the Cx hemichannel-related dye uptake of the cells as response to stimulation of adenosine receptors. The finding that NECA treatment also induced an increase in mRNA and protein levels of Cx26 is further evidence that the dye uptake was due to Cx26 hemichannels. It is of interest to note the following two observations: The stimulation of adenosine receptors downregulated Cx43 expression while upregulating Cx26 expression (Fig. 5A, B). The siRNA-dependent knockdown of Cx43 increased the expression of Cx26 and was followed by an increased activity of Cx hemichannels as documented by dye uptake experiments (Fig. 5C, D). The downregulation of Cx43 as result of NECA application could probably explain the reduction of gap junction coupling observed in the NECA-treated cells (Supplementary Fig. S2), indicating that while Cx26 was predominantly involved in hemichannel activity, Cx43 was mainly responsible for intercellular gap junction coupling. Future studies should clarify this point and the link between adenosine signalling and the downregulation of Cx43 and its consequence in respiratory airway epithelial cells. The upregulation of Cx26 expression in response to Cx43 knockdown suggests an antagonistic regulation of Cx26 and Cx43 expression that should be analysed more detailed in future studies.

Through activation of the A_{2A} and A_{2B} adenosine receptors expressed in Calu-3 cells, NECA upregulated the expression and synthesis of Cx26 (Fig. 5A), which correlated with an increase of Cx26 hemichannel activity (Fig. 4A). The increase of the hemichannel activity was suppressed when the adenosine receptor stimulation took place in the presence of MRS1754, an inhibitor of the A_{2B} adenosine receptor subtype, while the A_{2A} adenosine receptor subtype inhibitor SCH58261 did not affect the NECA-related enhancement of Cx hemichannel activity (Fig. 4E). Additionally, the A_{2A} adenosine receptor agonist CGS21680 was not able to significantly increase the dye uptake, while the specific A_{2B} adenosine receptor agonist BAY60-6583 was even slightly more efficient in increasing the dye uptake rate than NECA (Fig. 4E) [40]. Moreover, an analysis of the adenosine receptor expression showed that the A_{2B} adenosine receptor was more expressed than the A_{2A} adenosine receptor on mRNA level (Fig 4B). Similar results concerning adenosine receptor expression levels were found by other authors in bronchial epithelial cells [47]. Considering the results obtained through pharmacological modulation of adenosine receptors (Fig. 4E) and the expression data (Fig. 4B) we assume that the NECA-induced enhancement of Cx26 hemichannel activity was related to the stimulation of the A_{2B} adenosine receptor subtype. This assumption was confirmed by the finding that the NECA-related enhancement of Cx hemichannel activity was suppressed when the A_{2B} adenosine receptor subtype was knocked down using specific siRNA (Fig. 4F). From this it can be assumed that adenosine signalling affects Cx26 hemichannels only via the A_{2B} adenosine receptor subtype, the adenosine receptor subtype with the highest expression level, which agreed very well with other studies revealing that the A_{2B} adenosine receptor subtype was the most abundant adenosine receptor subtype in bronchial epithelial cells [48]. However, it is also possible that the different adenosine receptor subtypes may be linked to variable cascades, thereby regulating different functions [49]. In functional analyses the A_{2B} adenosine receptor was found in the whole cell membrane in an unpolarised manner [50–52]. For the A_{2A} adenosine receptor Sun et al. (2008) proposed an apical restriction of the localisation [50], while other authors argued for a strictly basolateral localisation [51, 52]. Regardless of these contradictions, these studies assume a polarization of the A_{2A} adenosine receptor subtype. The finding suggests that the A_{2A} and A_{2B} adenosine receptors might differ in their trafficking and probably in their scaffold systems to which they are anchored and thereby can be involved in different signalling cascades. Taken together the results show for the first time that stimulation of the A_{2B} adenosine receptor may specifically enhance Cx26 hemichannel activity in epithelial cells of the respiratory airway.

Concerning the pathway by which the activation of the A_{2B} adenosine receptor increased the Cx26 hemichannel activity (Fig. 6), we showed that the enhancement of Cx26 hemichannel activity was related to the activation of the cAMP/PKA cascade (Fig. 4C, D).

This signalling pathway can affect Cx channels by phosphorylation of Cxs [27, 28]. Cx26 was previously described as a non-phosphorylated Cx [28, 53], but new data show that Cx26 can be phosphorylated [54]. However, changes in phosphorylation take place within a short time in the range of minutes while the observed enhancement of Cx26 hemichannel activity was observable after stimulation period of many hours, suggesting that dependency to Cx26 phosphorylation for the observed effects was unlikely. Activation of the cAMP/PKA cascade can also regulate Cx expression [53]. Our results showed a significant increase of Cx26 and Cx30mRNA levels as a result of the stimulation of adenosine receptors using NECA (Fig. 5A), that was suppressed by inhibition of the PKA (Fig. 5A). An increase in the amount of specific mRNAs can be achieved by a transcriptional upregulation of the Cx26 and Cx30 genes or by a reduced mRNA degradation. We observed that the NECA-related increase of the cellular Cx26 mRNA content was antagonized by inhibition of the transcription factor Sp-1 (Fig. 5A). This result suggests that the increase of Cx26 and Cx30 mRNA content may be related to an upregulation of the respective gene transcription. Cx26 and Cx30 are encoded by the genes *GJB2* and *GJB6* in the deafness locus DFNB1 on 13q12 [55]. These genes are contiguous and co-regulation was observed in different cell types [56–58]. Interestingly, the upregulation of Cx26 correlated with a downregulation of Cx43 in Calu-3 cells (Fig. 5A). The mechanism of this finding is yet a matter of speculation. Expression of different Cxs is regulated by variable transcription factors [59]. The promotor regions of both the *GJB2* and *GJB6* gene contains binding sites of Sp1 [32, 60–63], a transcription factor which was shown to form a transcription complex with the PKA-activated cAMP response element-binding protein (CREB) [64]. Moreover, it was shown that depending on other co-expressed transcription factors, e.g. REV-ERBβ, Sp1 can upregulate or downregulate Cx43 expression [65]. Since the cAMP pathway participates in the expression of transcription factors [32, 66], it is tempting to speculate this was induced by activating cAMP synthesis through stimulation of A_{2B} adenosine receptors in epithelial cells of the respiratory airway, in turn upregulating the expression and synthesis of Cx26. The increasing amount of Cx26 proteins forming Cx26 hemichannels in the cell membrane thereby leads to an increase in Cx hemichannel activity (Fig. 6).

Persistent inflammation and alteration of lung structure are symptoms of chronic respiratory diseases, which encompass various pathological conditions such as cystic fibrosis (CF), idiopathic pulmonary fibrosis (IPF), COPD and asthma [67]. Adenosine is one of the mediators whose release is upregulated during inflammatory conditions of the respiratory airway epithelia [11, 21, 48]. Since we observed a possible adenosine-induced enhancement of Cx26 hemichannel activity through which intracellular molecules such as adenosine or purine nucleotides can be released, it is possible that adenosine signalling and Cx26 hemichannels interact in a vicious circle that fires and maintains the inflammation leading to detrimental effects in the tissue [19]. In this model (Fig. 6) a specific targeting of Cx26 could be a possible treatment of inflammation related diseases of the airway epithelium [23, 68].

Experiments were performed in the laboratory of A.N.. A.D, A.B. and A.N. contributed to the conception and design of the work as well as writing and revising the manuscript. A.D., T.L. and A.N. contributed to the acquisition, analysis, or interpretation of data for the work. A.B. provided technical support with gold nanoparticle-mediated laser perforation/dye transfer experiments and revised the work critically. All authors have approved the final version of the manuscript and agree to be accountable for all aspects of the work. All persons designated as authors qualify for authorship, and all those who qualify for authorship are listed.

The research was partly supported by the DFG project NG 4/10-1 and the BMBF project

The authors thank Nadine Dilger for technical support with the Cx-specific qRT-PCR primers and Patrik Schadzek for technical support with the dye uptake experiments. The authors also thank Klaudia Grieger for assistance with the experiments.

The authors have no conflicts of interest to declare.

1 Goodenough DA, Paul DL: Gap junctions. Cold Spring Harb Perspect Biol 2009;1:a002576.
2 Söhl G, Willecke K: Gap junctions and the connexin protein family. Cardiovasc Res 2004;62:228–232.
3 Berthoud VM, Beyer EC: Oxidative stress, lens gap junctions, and cataracts. Antioxid Redox Signal 2009;11:339–353.
4 Johnson RG, Le HC, Evenson K, Loberg SW, Myslajek TM, Prabhu A, Manley AM, O'Shea C, Grunenwald H, Haddican M, Fitzgerald PM, Robinson T, Cisterna BA, Sáez JC, Liu TF, Laird DW, Sheridan JD: Connexin Hemichannels: Methods for Dye Uptake and Leakage. J Membr Biol 2016;249:713–741.
5 Sáez JC, Retamal MA, Basilio D, Bukauskas FF, Bennett MVL: Connexin-based gap junction hemichannels: Gating mechanisms. Biochim Biophys Acta 2005;1711:215–224.
6 Maeda S, Tsukihara T: Structure of the gap junction channel and its implications for its biological functions. Cell Mol Life Sci 2011;68:1115–1129.
7 Schadzek P, Schlingmann B, Schaarschmidt F, Lindner J, Koval M, Heisterkamp A, Ngezahayo A, Preller M: Data of the molecular dynamics simulations of mutations in the human connexin46 docking interface. Data Brief 2016;7:93–99.
8 Orellana JA, Sánchez HA, Schalper KA, Figueroa V, Sáez JC: Regulation of intercellular calcium signaling through calcium interactions with connexin-based channels. Adv Exp Med Biol 2012;740:777–794.
9 Droguett K, Rios M, Carreño DV, Navarrete C, Fuentes C, Villalón M, Barrera NP: An autocrine ATP release mechanism regulates basal ciliary activity in airway epithelium. J Physiol 2017;595:4755–4767.
10 Blackburn MR, Vance CO, Morschl E, Wilson CN: Adenosine receptors and inflammation, in: Wilson CN, Mustafa SJ (eds): Adenosine receptors in health and disease; Handook of Experimental Pharmacology. Berlin, Heidelberg: Springer, 2009, vol. 193, pp 215–269.
11 Fredholm BB: Adenosine, an endogenous distress signal, modulates tissue damage and repair. Cell Death Differ 2007;14:1315–1323.
12 Eltzschig HK: Adenosine: An old drug newly discovered. Anesthesiology 2009;111:904–915.
13 Lazarowski ER, Tarran R, Grubb BR, van Heusden CA, Okada S, Boucher RC: Nucleotide release provides a mechanism for airway surface liquid homeostasis. J Biol Chem 2004;279:36855–6864.
14 Okada SF, Nicholas RA, Kreda SM, Lazarowski ER, Boucher RC: Physiological regulation of ATP release at the apical surface of human airway epithelia. J Biol Chem 2006;281:22992–23002.
15 Allen-Gipson DS, Wong J, Spurzem JR, Sisson JH, Wyatt TA: Adenosine A2A receptors promote adenosine-stimulated wound healing in bronchial epithelial cells. Am J Physiol Lung Cell Mol Physiol 2006;290:L849-855.
16 Lazarowski ER, Mason SJ, Clarke L, Harden TK, Boucher RC: Adenosine receptors on human airway epithelia and their relationship to chloride secretion. Br J Pharmacol 1992;106:774–782.
17 Alam MS, Costales MG, Cavanaugh C, Williams K: Extracellular adenosine generation in the regulation of pro-inflammatory responses and pathogen colonization. Biomolecules 2015;5:775–792.
18 Zuo P, Picher M, Okada SF, Lazarowski ER, Button B, Boucher RC, Elston TC: Mathematical model of nucleotide regulation on airway epithelia. Implications for airway homeostasis. J Biol Chem 2008;283:26805–26819.
19 Freund-Michel V, Muller B, Marthan R, Savineau JP, Guibert C: Expression and role of connexin-based gap junctions in pulmonary inflammatory diseases. Pharmacol Ther 2016;164:105–119.
20 Burnstock G: Purinergic Signalling: Therapeutic Developments. Front Pharmacol 2017;8:661.
21 Pelleg A, Schulman ES, Barnes PJ: Extracellular Adenosine 5'-Triphosphate in Obstructive Airway Diseases. Chest 2016;150:908–915.

22 Della Latta V, Cabiati M, Rocchiccioli S, Del Ry S, Morales MA: The role of the adenosinergic system in lung fibrosis. Pharmacol Res 2013;76:182–189.
23 Caruso M, Alamo A, Crisafulli E, Raciti C, Fisichella A, Polosa R: Adenosine signaling pathways as potential therapeutic targets in respiratory disease. Expert Opin Ther Targets 2013;17:761–772.
24 Cheng X, Ji Z, Tsalkova T, Mei F: Epac and PKA: A tale of two intracellular cAMP receptors. Acta Biochim Biophys Sin (Shanghai) 2008;40:651–662.
25 Bader A, Bintig W, Begandt D, Klett A, Siller IG, Gregor C, Schaarschmidt F, Weksler B, Romero I, Couraud PO, Hell SW, Ngezahayo A: Adenosine receptors regulate gap junction coupling of the human cerebral microvascular endothelial cells hCMEC/D3 by Ca2+ influx through cyclic nucleotide-gated channels. J Physiol 2017;595:2497–2517.
26 Begandt D, Bintig W, Oberheide K, Schlie S, Ngezahayo A: Dipyridamole increases gap junction coupling in bovine GM-7373 aortic endothelial cells by a cAMP-protein kinase A dependent pathway. J Bioenerg Biomembr 2010;42:79–84.
27 Lampe PD, Lau AF: The effects of connexin phosphorylation on gap junctional communication. Int J Biochem Cell Biol 2004;36:1171–1186.
28 Laird DW: Connexin phosphorylation as a regulatory event linked to gap junction internalization and degradation. Biochim Biophys Acta 2005;1711:172–182.
29 Dukic AR, Haugen LH, Pidoux G, Leithe E, Bakke O, Taskén K: A protein kinase A-ezrin complex regulates connexin 43 gap junction communication in liver epithelial cells. Cell Signal 2017;32:1–11.
30 Ampey BC, Morschauser TJ, Lampe PD, Magness RR: Gap junction regulation of vascular tone: Implications of modulatory intercellular communication during gestation. Adv Exp Med Biol 2014;814:117–132.
31 Zhang F, Cheng J, Lam G, Jin DK, Vincent L, Hackett NR, Wang S, Young LM, Hempstead B, Crystal RG, Rafii S: Adenovirus vector E4 gene regulates connexin 40 and 43 expression in endothelial cells via PKA and PI3K signal pathways. Circ Res 2005;96:950–957.
32 Rohlff C, Ahmad S, Borellini F, Lei J, Glazer RI: Modulation of transcription factor Sp1 by cAMP-dependent protein kinase. J Biol Chem 1997;272:21137–21141.
33 Foster KA, Avery ML, Yazdanian M, Audus KL: Characterization of the Calu-3 cell line as a tool to screen pulmonary drug delivery. Int J Pharm 2000;208:1–11.
34 Zhang Y, Reenstra WW, Chidekel A: Antibacterial activity of apical surface fluid from the human airway cell line Calu-3: Pharmacologic alteration by corticosteroids and beta(2)-agonists. Am J Respir Cell Mol Biol 2001;25:196–202.
35 Shen BQ, Finkbeiner WE, Wine JJ, Mrsny RJ, Widdicombe JH: Calu-3: A human airway epithelial cell line that shows cAMP-dependent Cl- secretion. Am J Physiol 1994;266:L493-501.
36 Begandt D, Bader A, Antonopoulos GC, Schomaker M, Kalies S, Meyer H, Ripken T, Ngezahayo A: Gold nanoparticle-mediated (GNOME) laser perforation: A new method for a high-throughput analysis of gap junction intercellular coupling. J Bioenerg Biomembr 2015;47:441–449.
37 Heinemann D, Schomaker M, Kalies S, Schieck M, Carlson R, Murua Escobar H, Ripken T, Meyer H, Heisterkamp A: Gold nanoparticle mediated laser transfection for efficient siRNA mediated gene knock down. PloS one 2013;8:e58604.
38 Schadzek P, Stahl Y, Preller M, Ngezahayo A: Analysis of the dominant mutation N188T of human connexin46 (hCx46) using concatenation and molecular dynamics simulation. FEBS Open Bio 2019;9:840–850.
39 Grainger CI, Greenwell LL, Lockley DJ, Martin GP, Forbes B: Culture of Calu-3 cells at the air interface provides a representative model of the airway epithelial barrier. Pharm Res 2006;23:1482–1490.
40 Klotz KN: Adenosine receptors and their ligands. Naunyn Schmiedebergs Arch Pharmacol 2000;362:382–391.
41 Koval M: Claudin heterogeneity and control of lung tight junctions. Acta Biochim Biophys Sin (Shanghai) 2013;75:551–567.
42 Eckle T, Koeppen M, Eltzschig HK: Role of extracellular adenosine in acute lung injury. Physiology (Bethesda) 2009;24:298–306.
43 Chunn JL, Young HW, Banerjee SK, Colasurdo GN, Blackburn MR: Adenosine-dependent airway inflammation and hyperresponsiveness in partially adenosine deaminase-deficient mice. J Immunol 2001;167:4676–4685.
44 Frank JA: Claudins and alveolar epithelial barrier function in the lung. Ann NY Acad Sci 2012;1257:175–183.

45 Patel D, Zhang X, Veenstra RD: Connexin hemichannel and pannexin channel electrophysiology: How do they differ? FEBS Lett 2014;588:1372–1378.
46 Pan F, Mills SL, Massey SC: Screening of gap junction antagonists on dye coupling in the rabbit retina. Vis Neurosci 2007;24:609–618.
47 Davis CW, Lazarowski E: Coupling of airway ciliary activity and mucin secretion to mechanical stresses by purinergic signaling. Respir Physiol Neurobiol 2008;163:208–213.
48 Sun C-X, Zhong H, Mohsenin A, Morschl E, Chunn JL, Molina JG, Belardinelli L, Zeng D, Blackburn MR: Role of A2B adenosine receptor signaling in adenosine-dependent pulmonary inflammation and injury. J Clin Invest 2006;116:2173–2182.
49 Gao ZG, Inoue A, Jacobson KA: On the G protein-coupling selectivity of the native A2B adenosine receptor. Biochem Pharmacol 2018;151:201–213.
50 Sun Y, Wu F, Sun F, Huang P: Adenosine promotes IL-6 release in airway epithelia. J Immunol 2008;180:4173–4181.
51 Szkotak AJ, Ng AML, Man SFP, Baldwin SA, Cass CE, Young JD, Duszyk M: Coupling of CFTR-mediated anion secretion to nucleoside transporters and adenosine homeostasis in Calu-3 cells. J Membr Biol 2003;192:169–179.
52 Wang D, Sun Y, Zhang W, Huang P: Apical adenosine regulates basolateral Ca2+-activated potassium channels in human airway Calu-3 epithelial cells. Am J Physiol Cell Physiol 2008;294:C1443-1453.
53 Traub O, Look J, Dermietzel R, Brümmer F, Hülser D, Willecke K: Comparative characterization of the 21-kD and 26-kD gap junction proteins in murine liver and cultured hepatocytes. J Cell Biol 1989;108:1039–1051.
54 Locke D, Bian S, Li H, Harris AL: Post-translational modifications of connexin26 revealed by mass spectrometry. Biochem J 2009;424:385–398.
55 Guilford P, Ben Arab S, Blanchard S, Levilliers J, Weissenbach J, Belkahia A, Petit C: A non-syndrome form of neurosensory, recessive deafness maps to the pericentromeric region of chromosome 13q. Nat Genet 1994;6:24–28.
56 Ortolano S, Di Pasquale G, Crispino G, Anselmi F, Mammano F, Chiorini JA: Coordinated control of connexin 26 and connexin 30 at the regulatory and functional level in the inner ear. Proc Natl Acad Sci U S A 2008;105:18776–18781.
57 Boulay AC, del Castillo FJ, Giraudet F, Hamard G, Giaume C, Petit C, Avan P, Cohen-Salmon M: Hearing is normal without connexin30. J Neurosci 2013;33:430–434.
58 Kelly JJ, Abitbol JM, Hulme S, Press ER, Laird DW, Allman BL: The connexin 30 A88V mutant reduces cochlear gap junction expression and confers long-term protection against hearing loss. J Cell Sci 2019;132:pii:jcs224097.
59 Oyamada M, Takebe K, Oyamada Y: Regulation of connexin expression by transcription factors and epigenetic mechanisms. Biochim Biophys Acta 2013;1828:118–133.
60 del Castillo FJ, Del Castillo I: DFNB1 Non-syndromic Hearing Impairment: Diversity of Mutations and Associated Phenotypes. Front Mol Neurosci 2017;10:428.
61 Kiang DT, Jin N, Tu ZJ, Lin HH: Upstream genomic sequence of the human connexin26 gene. Gene 1997;199:165–171.
62 Tu ZJ, Kollander R, Kiang DT: Differential up-regulation of gap junction connexin 26 gene in mammary and uterine tissues: The role of Sp transcription factors. Mol Endocrinol 1998;12:1931–1938.
63 Tu ZJ, Kiang DT: Mapping and characterization of the basal promoter of the human connexin26 gene. Biochim Biophys Acta 1998;1443:169–181.
64 Mukherjee S, Sengupta Bandyopadhyay S: Mechanism of prostaglandin E2-induced transcriptional up-regulation of Oncostatin-M by CREB and Sp1. Biochem J 2018;475:477–494.
65 Negoro H, Okinami T, Kanematsu A, Imamura M, Tabata Y, Ogawa O: Role of Rev-erbα domains for transactivation of the connexin43 promoter with Sp1. FEBS Lett 2013;587:98–103.
66 Li L, Zhang Z, Peng J, Wang Y, Zhu Q: Cooperation of luteinizing hormone signaling pathways in preovulatory avian follicles regulates circadian clock expression in granulosa cell. Mol Cell Biochem 2014;394:31–41.
67 Stolzenburg LR, Harris A: The role of microRNAs in chronic respiratory disease: Recent insights. Biol Chem 2018;399:219–234.
68 Willebrords J, Maes M, Crespo Yanguas S, Vinken M: Inhibitors of connexin and pannexin channels as potential therapeutics. Pharmacol Ther 2017;180:144–160.